

Spin-Parity Analysis of the Centrally Produced $K_S^0 K^\pm \pi^\mp$ System at 800 GeV/c

M. Sosa,¹ M. C. Berisso,² D. C. Christian,³ J. Félix,¹ A. Gara,^{4,*} E. Gottschalk,^{4,†} G. Gutiérrez,³ E. P. Hartouni,^{2,‡}
 B. C. Knapp,⁴ M. N. Kreisler,^{2,‡} S. Lee,^{2,§} K. Markianos,^{2,||} G. Moreno,¹ M. A. Reyes,^{1,¶} M. Wang,^{2,‡}
 A. Wehmann,³ and D. Wesson^{2,**}

¹Universidad de Guanajuato, León, Guanajuato, México

²University of Massachusetts, Amherst, Massachusetts 01003

³Fermilab, Batavia, Illinois 60510

⁴Columbia University, Nevis Laboratories, Irvington, New York 10533

(Received 31 July 1997; revised manuscript received 6 April 1999)

Results are presented from an analysis of a large sample of centrally produced mesons in the reaction $pp \rightarrow p_{\text{slow}}(K_S^0 K^\pm \pi^\mp) p_{\text{fast}}$ with 800 GeV/c protons incident on liquid hydrogen. Two resonances dominate the final state, the $f_1(1285)$, decaying into $a_0 \pi$, and the $f_1(1420)$, decaying into $K^* K$. Both mesons are produced with equal amounts of $|J_z|^\eta = 1^\pm$, and no $J_z = 0$.

PACS numbers: 14.40.Cs, 11.80.Et, 12.39.Mk, 13.85.Hd

For many years, the classification of mesons decaying into $K\bar{K}\pi$ has been problematic. The observed spectrum depends dramatically on the production mechanism, but not in a way which is easily understood. The confusing aspects of the spectrum have been called “the E/ι puzzle [1,2].” In the mass region just above 1400 MeV/c², at least two pseudoscalars are seen in J/ψ decays, and in a variety of hadronic interactions. This region also contains two 1^{++} mesons, the $f_1(1420)$ [3–5], and the $f_1(1510)$ [6]. If confirmed, the $f_1(1510)$, seen in $K^- p$ interactions, would be the $s\bar{s}$ partner of the $f_1(1285)$, leaving the $f_1(1420)$ as a non- $q\bar{q}$ candidate [1]. In this paper, we report the results of an analysis of the $K\bar{K}\pi$ system produced in a high statistics study of pp central production in the doubly diffractive reaction,

$$pp \rightarrow p_{\text{slow}}(K_S^0 K^\pm \pi^\mp) p_{\text{fast}}, \quad K_S^0 \rightarrow \pi^+ \pi^- . \quad (1)$$

This study was motivated in part by the possibility that the production of non- $q\bar{q}$ mesons may be favored in central production.

The results presented here are based on an analysis of 10% of the 5×10^9 events recorded by Fermilab E690 during Fermilab’s 1991 fixed target run. The E690 apparatus consisted of a high rate, open geometry multiparticle spectrometer (Fig. 1) used to measure the target system (T) in $pp \rightarrow p_{\text{fast}}(T)$ reactions, and a beam spectrometer system used to measure the incident 800 GeV/c beam and scattered proton. A liquid hydrogen target was located just upstream of the multiparticle spectrometer. The 96 cell Cherenkov counter located at the downstream end of the main spectrometer magnet used freon 114 as a radiator and had a pion threshold of 2.57 GeV/c. The E690 apparatus has been described elsewhere [7].

Reaction (1) was selected by requiring a primary vertex in the LH_2 target with one positive track, one negative track, a K_S^0 , an incoming beam track, and a fast forward proton. At least one of the two charged tracks was required to be identified by the Cherenkov counter as either a π , or an ambiguous K/p . The other track was

required to have an identity compatible with the final state. No direct measurement was made of the slow proton. The missing mass squared shown in Fig. 2 has a clear proton peak for both charge states of reaction (1); the selected events are shaded.

In all selected events, the forward proton, p_{fast} , was separated from the central mesons by at least 3.5 units of rapidity. This was due to limited multiparticle detection and reconstruction efficiency for high momentum tracks.

A minimum gap of 1.8 units of rapidity was required between each individual meson and p_{slow} . This ensured that there was no contamination of the final state from reactions in which p_{slow} was a decay product of a baryon resonance, such as Δ^{++} or $\Lambda(1520)$. Finally, in order to ensure near uniform acceptance, the x_F of the meson system was required to be in the range $[-0.15, -0.02]$.

Figures 2(a) and 2(c) show the $K\bar{K}\pi$ invariant mass distributions for the selected data sample. In both charge states, the spectrum is dominated by two peaks. One of these is easily identified by its mass and width as the $f_1(1285)$. The second peak has a central value of

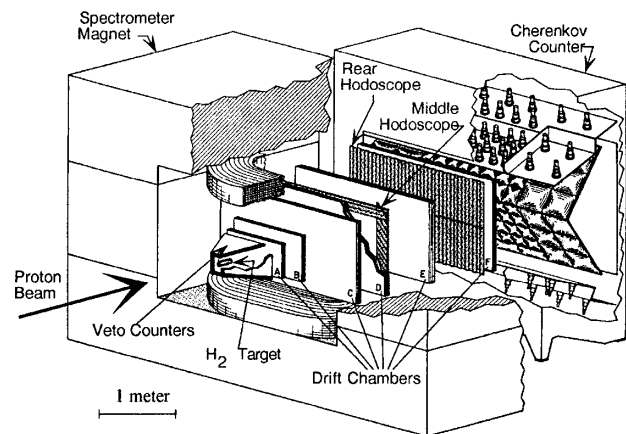


FIG. 1. E690 multiparticle spectrometer.

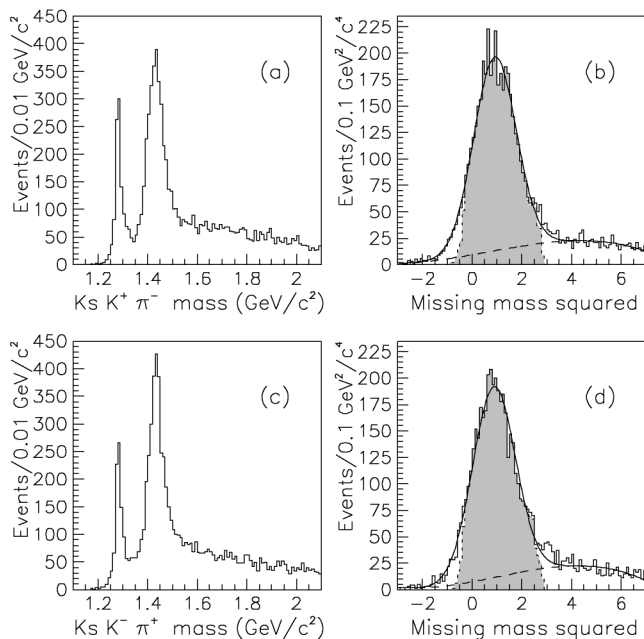


FIG. 2. (a) Invariant mass and (b) Missing mass squared between threshold and 1480 MeV/c² for $K_S^0 K^+ \pi^-$. (c) Invariant mass and (d) missing mass squared between threshold and 1480 MeV/c² for $K_S^0 K^- \pi^+$.

1430 MeV/c². The rms mass resolutions at 1285 and 1430 MeV/c² are 1.1 and 1.5 MeV/c², respectively. No obvious structure is seen at higher mass. In particular, the $f_1(1510)$ seen in $K^- p$ interactions [6] is not evident.

The plots in Fig. 3 show the Dalitz distribution for the $K_S^0 K^+ \pi^-$ data in the mass range 1390–1480 MeV/c² (upper left), and the Monte Carlo (MC) Dalitz distributions for $J = 0, 1$ states decaying into $K^* K$ and $a_0 \pi$. Examination of these Dalitz plots shows that the peak at

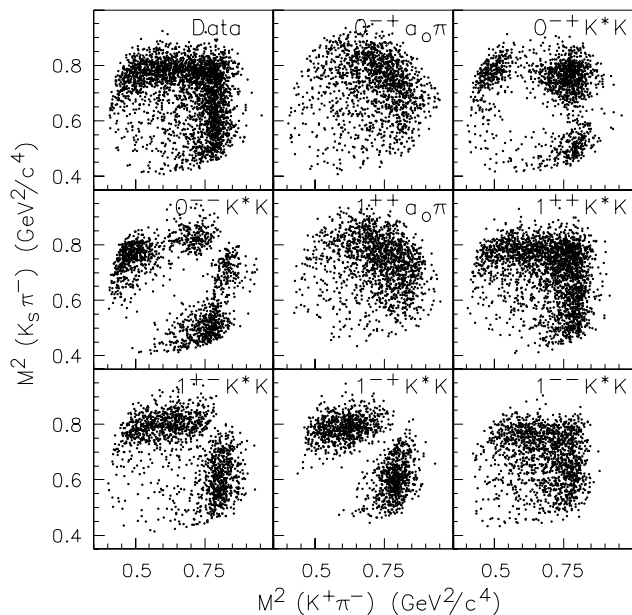


FIG. 3. Dalitz plots for both data and MC for the $K_S^0 K^+ \pi^-$ system.

1430 MeV/c² in the data is almost certainly dominated by decays of a single 1^{++} meson, the $f_1(1420)$, into the final state $K^* K$. The $K_S^0 K^- \pi^+$ Dalitz distribution (not shown) is also clearly dominated by $1^{++} K^* K$ decays.

In order to confirm the conclusions reached by the inspection of the invariant mass distributions and Dalitz plots, and to reveal more subtle features of the spectra, a partial wave analysis was performed. The analysis assumed a two step process: the production step in which a meson system was formed by the collision of two objects emitted by the scattered protons, and the decay step in which the meson system decayed into $K \bar{K} \pi$. The decay was also assumed to occur in two steps: a two body decay to either $a_0 \pi$ or $K^* K$, followed by the decay of the a_0 or K^* isobar. The analysis was done using the BNL Multiparticle Spectrometer parametrization [8]. Waves were labeled with spin, parity, and G parity J^{PG} , the isobar, and the absolute value of the spin projection and naturality $|J_z|^\eta$. All waves with spin 0 and 1 and isobars K^* and a_0 were tried. As Figs. 2(b) and 2(d) show, in the region between threshold and 1480 MeV/c² the background is small. Therefore, an incoherent background was not included in the fit.

The $K^*(892)$ isobar was parametrized by a relativistic Breit-Wigner function, with mass and width as listed by the Particle Data Group [1]. The parametrization given in [8] was used for the $a_0(980)$.

The production coordinate system was defined in the $K \bar{K} \pi$ center of mass, with the y axis perpendicular to the plane formed by $\vec{p}_{fast} - \vec{p}_{beam}$ and $\vec{p}_{slow} - \vec{p}_{target}$ in the pp center of mass, and the z axis in the direction of $\vec{p}_{fast} - \vec{p}_{beam}$ in the $K \bar{K} \pi$ center of mass. The decay of the meson system was characterized by its isobar mass, the polar and azimuthal angles (θ, ϕ) of the bachelor particle in the $K \bar{K} \pi$ center of mass, and the polar and azimuthal angles (α, γ) of the K^\pm in the isobar center of mass. The isobar coordinate system was defined by a Lorentz boost from the $K \bar{K} \pi$ center of mass

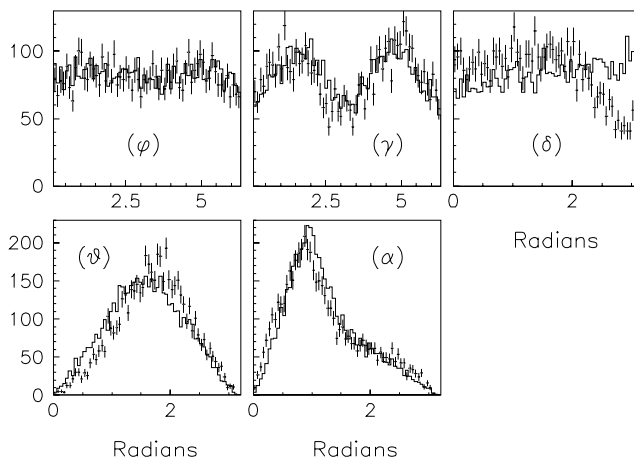


FIG. 4. Angular distributions for data (error bars) and $1^{++} K^* K$ MC (histograms) for the $K_S^0 K^\pm \pi^\mp$ system in the mass range 1390–1480 MeV/c².

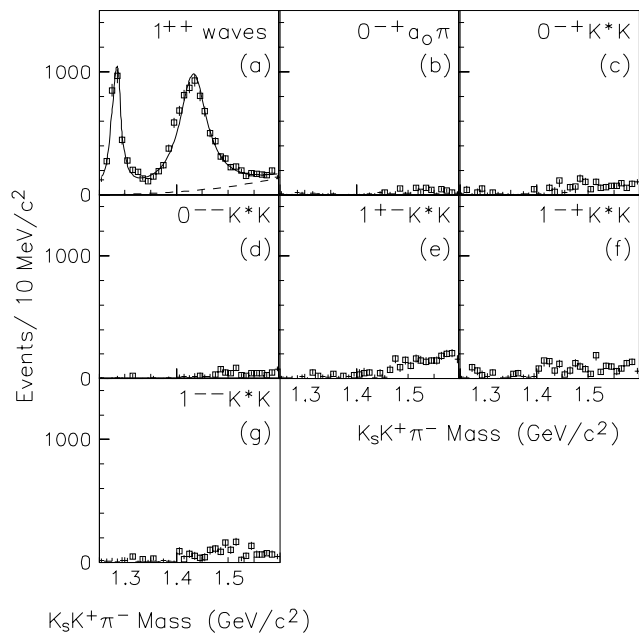


FIG. 5. Partial wave intensities for the $K_S^0 K^+ \pi^-$ system. The waves (b) to (g) were added one at a time to the waves (a). The fit in (a) is described in the text.

to the isobar center of mass. The angle between the $p_{\text{beam}}-p_{\text{fast}}$ and the $p_{\text{target}}-p_{\text{slow}}$ scattering planes in the $K\bar{K}\pi$ center of mass is labeled δ . Figure 4 shows these angular distributions for data (error bars) and Monte Carlo (histograms) for the $K_S^0 K^\pm \pi^\mp$ final state in the mass range 1390–1480 MeV/c^2 . The Monte Carlo events were generated with a pure $1^{++} K^* K$ state with $|J_z|^\eta = 1^\pm$ (no $J_z = 0$) components. δ was generated flat in the

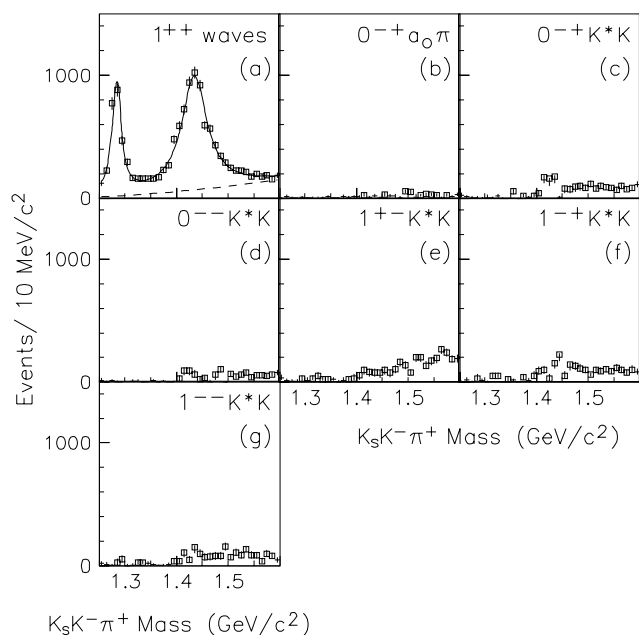


FIG. 6. Partial wave intensities for the $K_S^0 K^- \pi^+$ system. The waves (b) to (g) were added one at a time to the waves (a). The fit in (a) is described in the text.

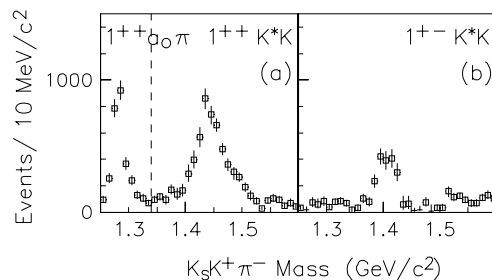


FIG. 7. Partial wave intensities for the $K_S^0 K^+ \pi^-$ system when the $1^{+-} K^* K$ waves are added to the $1^{++} a_0 \pi$ waves below 1340 MeV/c^2 , and to the $1^{++} K^* K$ waves above 1340 MeV/c^2 .

pp center of mass. A good agreement between data and Monte Carlo for the angles $(\phi, \theta, \gamma, \alpha)$ is observed. The angle δ is not used in the partial wave analysis.

The wave amplitudes were determined by maximizing the log of the extended likelihood function [9], using a density matrix of rank one [10]. The analysis was done in 10 MeV/c^2 bins of $K\bar{K}\pi$ mass, from threshold to 1600 MeV/c^2 , with x_F restricted to the range $[-0.15, -0.02]$, and integrated over p_t^2 for both protons, and over the angle δ between the two proton scattering planes in the $K\bar{K}\pi$ center of mass. Monte Carlo events were used to calculate acceptance integrals. These integrals were calculated for each mass bin using a flat x_F distribution. Events were generated using an $e^{-\alpha p_t^2}$ distribution for each scattered proton, with $\alpha = 6.5$ for p_{slow} , and $\alpha = 7.5$ for p_{fast} (to match the observed distributions).

The partial wave analysis was performed for each mass bin separately. Each of the 18 waves was tried one at a time. The wave that maximized the likelihood was kept, and each of the remaining 17 waves added to it one at a time. The two wave solution that maximized the likelihood was kept for the third iteration, and each of the remaining 16 waves added one at a time. This process of adding one wave per iteration was continued

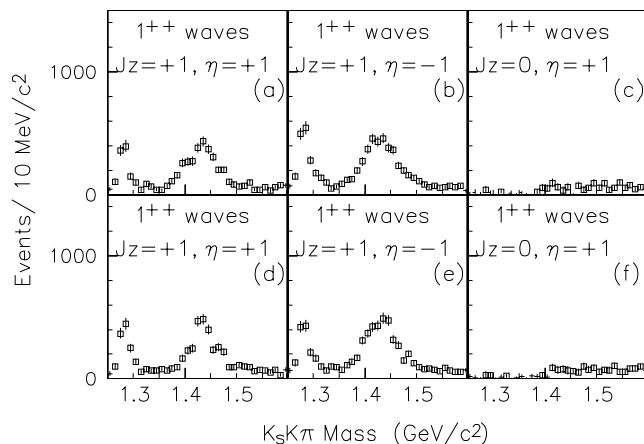


FIG. 8. Separate $|J_z|^\eta$ partial wave intensities. (a)–(c) For the $K_S^0 K^+ \pi^-$ system. (d)–(f) For the $K_S^0 K^- \pi^+$ system.

TABLE I. Masses and widths given by the fit.

Decay	Mass (MeV/c ²)	Width (MeV/c ²)
$K_S^0 K^+ \pi^-$	1281.9 ± 0.5	18.2 ± 1.2
	1430.8 ± 0.9	68.7 ± 2.9
$K_S^0 K^- \pi^+$	1282.8 ± 0.6	19.4 ± 1.5
	1433.4 ± 0.8	58.8 ± 3.3

until the maximum change (in any mass bin) of the log of the likelihood was less than 3 units.

Below 1340 MeV/c², only the two $1^{++} a_0 \pi$ waves with $|J_z|^\eta = 1^\pm$ [the $f_1(1285)$] were required. Above 1340 MeV/c², four dominant waves were needed: the two $1^{++} K^* K$ waves with $|J_z|^\eta = 1^\pm$ [the $f_1(1420)$], and the two $1^{++} a_0 \pi$, $|J_z|^\eta = 1^\pm$ waves. The sums of intensity for these waves are shown in Figs. 5(a) and 6(a). Since the $1^{++} K^* K$ and $1^{++} a_0 \pi$ waves are not orthogonal, their intensities cannot be shown separately [11]. The $1^{++} a_0 \pi$ waves above 1340 MeV/c² could be due to the tail of the $f_1(1285)$ or to decays of the $f_1(1420)$ into $a_0 \pi$ with a small branching fraction compared to the $K^* K$ decays [4]. In Figs. 5 and 6, the acceptance corrected intensities (normalized to the number of events) are shown for each set of waves. For spin one, the figures show a sum of the $|J_z|^\eta$ components. In each case, one additional wave was added to the waves in Figs. 5(a) and 6(a). When the $1^{++} a_0 \pi$ waves are not included above 1340 MeV/c², a strong peak in the $1^{+-} K^* K$ waves appears at 1400 MeV/c², as shown in Fig. 7 for the $K_S^0 K^+ \pi^-$ data set [12]. This artifact also appears in the $K_S^0 K^- \pi^+$ amplitudes when the $1^{++} a_0 \pi$ waves are not included above 1340 MeV/c².

A best fit to the data shown in Figs. 5(a) and 6(a) was performed using two nonrelativistic Breit-Wigner functions plus a background parametrized as $a(m - m_{th})^b$, where m is the $K\bar{K}\pi$ effective mass, m_{th} is the $K\bar{K}\pi$ threshold, and a and b are fit parameters. The results are shown in Table I. The errors are statistical only.

As stated above, the data can be described completely using only waves with $|J_z|^\eta = 1^\pm$. This striking result is shown in Fig. 8, which shows the intensities using six $|J_z|^\eta = 1^\pm, 0^+$ $K^* K$ and $a_0 \pi$ waves. For both states, the solution contains equal amounts of $|J_z|^\eta = 1^\pm$, and no $|J_z| = 0$. This may be a consequence of the production mechanism [13]. If a meson of spin J is formed by the interaction of two identical particles of helicities λ_1 and λ_2 , then the production amplitude $F_{\lambda_1 \lambda_2}^J = (-1)^J F_{\lambda_2 \lambda_1}^J$. Therefore $J = 1 \Rightarrow \lambda_1 \neq \lambda_2 \Rightarrow J_z = \lambda_1 - \lambda_2 \neq 0$.

In summary, results have been presented from a high statistics study of the centrally produced $K\bar{K}\pi$ system. Two resonances dominate the final state, the $f_1(1285)$, and the $f_1(1420)$. This confirms previous results that pseudoscalar states are not seen in the central production

of $K\bar{K}\pi$ [3]. The f_1 mesons are produced spin aligned; both $|J_z|^\eta = 1^\pm$ components are seen with equal strength, and in each case, the $|J_z| = 0$ component is absent.

We thank S. U. Chung, A. Kirk, and M. Albrow for useful discussions. This work was funded in part by the Department of Energy under Contracts No. DE-AC02-76CHO3000 and No. DE-AS05-87ER40356, the National Science Foundation under Grants No. PHY89-21320 and No. PHY90-14879, and CONACyT de Mexico under Grants No. 1061-E9201 and No. 3793-E9401.

*Present address: IBM Corp., Yorktown Heights, NY, 10598.

†Present address: Fermilab, Batavia, IL, 60510.

‡Present address: LLNL, Livermore, CA, 94551.

§Present address: Cognex Corp., Natic, MA, 01760.

||Present address: University of Washington, Seattle, WA, 98109.

¶Present address: Universidad of Michoacana, Morelia, Mexico.

**Present address: OAO Corp., Athens, GA, 30605.

- [1] Particle Data Group, R. M. Barnett *et al.*, Phys. Rev. D **54**, 1 (1996); Particle Data Group, C. Caso *et al.*, Eur. Phys. J. C **3**, 1 (1998).
- [2] F. Nichitiu, in *Proceedings of Hadron'95*, edited by M. C. Birse, G. D. Lafferty, and J. A. McGovern (World Scientific, Singapore, 1996), p. 164; A. Lanaro, Nucl. Phys. B, Proc. Suppl. **56A**, 136 (1997).
- [3] T. A. Armstrong *et al.*, Phys. Lett. **146B**, 273 (1984); Z. Phys. C **34**, 23 (1987); Phys. Lett. B **221**, 216 (1989); Z. Phys. C **56**, 29 (1992).
- [4] D. Barberis *et al.*, Phys. Lett. B **440**, 225 (1998).
- [5] H. Aihara *et al.*, Phys. Rev. Lett. **57**, 2500 (1986); G. Gidal *et al.*, Phys. Rev. Lett. **59**, 2016 (1987).
- [6] D. Aston *et al.*, Phys. Lett. B **201**, 573 (1988); P. Gavillet *et al.*, Z. Phys. C **16**, 119 (1982).
- [7] The E690 spectrometer previously used in BNL E766 is described in J. Uribe *et al.*, Phys. Rev. D **49**, 4373 (1994). The beam chambers are described in D. C. Christian *et al.*, Nucl. Instrum. Methods Phys. Res., Sect. A **345**, 62 (1994).
- [8] S. U. Chung, "Formulas for Partial Wave Analysis," BNL Report, 1989; S. K. Blessing, Ph.D. thesis, Indiana University, 1988.
- [9] M. Sosa, Ph.D. thesis, Universidad de Guanajuato, México, 1996.
- [10] S. U. Chung and T. L. Trueman, Phys. Rev. D **11**, 633 (1975).
- [11] D. Aston, T. A. Lasinski, and P. K. Sinervo, Report No. SLAC-R-287, SLAC 1985.
- [12] At 1400 MeV/c², the solution including the $1^{++} a_0 \pi$ waves is preferred over this solution (including the $1^{+-} K^* K$ waves) by 60 units of ln(likelihood).
- [13] This explanation was suggested by S. U. Chung; S. U. Chung, CERN Yellow Report No. CERN 71-8, 1971; F. E. Close, Phys. Lett. B **419**, 387 (1998).